Slutrapport BVFF

BVFF nummer:

2016-025

Projekttitel

Biomekanisk optimering av stötdämpande beläggning som fallskadeprevention för fotgängare och cyklister

Slutrapport på Engelska

Svein Kleiven, Pooya Sahandifar, Viveca Wallqvist

Abstract

A fall is a serious health issue for the elderly. Among different fall types, the sideways fall is considered to be more severe concerning the injury outcome. When elderlies experience an unintentional sideways fall, they can either resist the impact forces with the soft tissue force attenuation capacity and femoral strength or need external protections to reduce the injury risk. In this project, these two aspects were investigated. Finite element whole-body models are valuable instruments for analyzing the fall biomechanics and investigating the possible preventive measures more conveniently. The whole-body models were developed to investigate the traffic accidents; however, a sideways fall has different kinematics than the other types of accidents. Consequently, it is necessary to enhance the whole-body models according to the major fall parameters, leading to severe injury cases, before assessing the external protection capabilities.

The current project attempted to advance these two critical aspects regarding the fall induced injuries. A finite element whole-body model was chosen to study three critical parameters in the fall biomechanics: body posture, soft tissue, femoral strength. The whole body model was positioned in different body configurations relevant for the sideways fall to evaluate the body posture that leads to the highest internal forces on the femoral head. Next, different soft tissue constitutive material models and soft tissue thicknesses were investigated to find a material model that could accurately reproduce the experimental results according to an objective rating method named CORA. Finally, the separate and combined effects of geometrical and mechanical properties changes due to aging on the femoral strength were assessed for the elderly males and females. In the second aspect of the project, the shock-absorbing rubberized asphalt pavements' preventive capacity was examined. First, different rubberized asphalt mixtures were implemented in bicycle and pedestrian accident reconstructions to evaluate the head injury risks. Later, the asphalt mixtures were studied in the sideways fall incidents to evaluate the hip fracture risk in elderly medium-size males and small-size females.

The first aspect of the project presented the results and methods to improve the sideways fall analysis, and the second aspect of the project focused on assessing the rubberized asphalt mixtures for injury prevention purposes. The sideways falls with the upright trunk, and a slightly forward-tilted pelvis could lead to the highest internal forces. A nonlinear Ogden material model scored better among different soft tissue material models in the side impacts to the hip segments. The geometrical and mechanical properties changes due to aging lead to a different behavior for males and females. Females experience a higher rate of strength loss due to aging. Moreover, it was indicated that a rubberized asphalt mixture could reduce the head injury risk for pedestrians and cyclists and the hip fracture risk for the elderly. The amount of rubber in the asphalt mixtures needs to exceed a specific limit to observe rubberized asphalts' preventive effects. Consequently, it is necessary to optimize the mixtures' rubber content to improve its prevention capacity.

In summary, the current project presented a method to improve the whole-body models according to the sideways fall requirements and assessed the protective capacity of the rubberized asphalt mixtures in head and hip injuries.

1 Introduction

A fall injury can cause fracture or laceration in different body segments but usually, forward and backward falls lead to wrist and upper extremity injuries, while sideways falls lead to hip fractures [1]. Figure 1.1 shortly summarizes the fall-induced injuries with their frequency and severity. Among fall-induced injuries, the hip fractures are more severe among elderly, since it causes loss of mobility, higher mortality rate, and social and economic costs [2], [3]. Old female adults have a higher risk of hip fracture due to the increased bone loss and falling frequency [4]–[6].

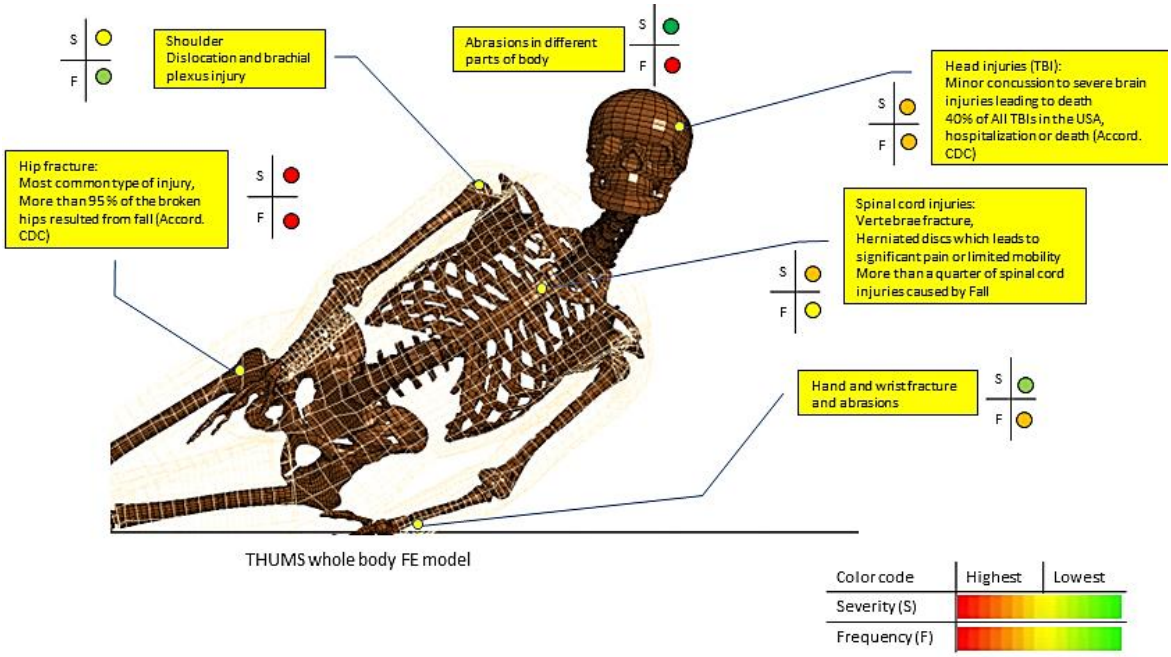

Figure 1.1. Summary of possible fall-induced injuries according to previous studies [1], [7].

According to the Swedish transport administration, pedestrians falling outdoors and cyclists account for about 70 percent of severe injuries in road traffic environments [8]. Another study on traffic fatality of 31 major cities globally suggests that pedestrians and cyclists consist of half of the fatalities [9]. Despite the improvements in traffic accident preventions during past decades [10], cyclists and pedestrians, or more broadly vulnerable road users (VRU), received less attention [9]. Cyclists can enjoy better protection by wearing helmets [11], [12]; however, there is no specific protection for the pedestrians.

Older adults reduce their outdoor activities as they age. Part of the reduced activity is the fear of falling. In addition to older adults, pedestrians from other demographics are also at risk of falling outdoors. A beneficial measure to reduce the risk of injury for pedestrians could be compliant shock-absorbing pavements. Only a few studies investigated the effect of reducing the stiffness of the asphalt mixtures (Figure 1.2) on reducing head injury risk [13], [14]. A previous study on several asphalt mixtures suggests a 45% reduction in skull fracture risk in an asphalt mixture containing 60%vol. rubber [13].

Figure 1.2. Rubber asphalt mixture (left), rubber concrete casting (right) [13] (Licence acquired through Copyright Clearance Center).

The finite element method is a numerical method that could be used to evaluate the potential capability of a proposed solution for reducing the risk of injury. This method is widely used for traffic accident reconstructions and various accidents [15]–[20]. It included several forms of accidents, such as single-vehicle accidents and vehicle-pedestrian accidents, but not fall accidents.

2 Objectives

The project's main objective was to better understand the fall-induced injury biomechanics better using the THUMS whole-body model and evaluate the rubberized asphalt pavements' capacity to reduce the risk of head injuries and hip fractures.

Two main questions were asked in the definition of each study within the project:

- How do different parameters such as age influence the fall injury biomechanics?
- Does the proposed idea of a compliant pavement reduce the risk of major fall injuries, i.e., hip fracture and head injury?

The first question was addressed in the papers A, B, and C and the second question was addressed in the papers D and E.

The specific aim of each study was as follows:

Paper A To evaluate the effect of body configuration, the trunk angle (the angle between the trunk and vertical) and the pelvis angle (anterior and posterior rotation of the pelvis), on the internal forces on the femoral head induced from the sideways falls.

Paper B To investigate the effect of soft tissue material modeling on the external and internal forces applied to the femur during sideways falls using an objective CORrelation and Analysis (CORA) method.

Paper C To study the separate and combined effect of geometrical and mechanical properties changes due to aging on femoral strength.

The second aspect of the project was examined. It was hypothesized that a more compliant asphalt mixture could potentially reduce the risk of injury. The aim of the designed studies was as follows:

Paper D To assess the effect of varying rubber content in the rubberized asphalt samples to reduce head injury risk using a bicycle and a pedestrian accident case.

Paper E To evaluate the rubberized asphalt mixture's capability in reducing the risk of sideways falls hip injury.

3 Background

The majority of hip fractures happens because of a fall [1], [21]. A previous study [22] suggested four conditions that a fall results in a hip fracture if it is satisfied: (i) The fall occurs close to the pelvis segment, (ii) the fall cannot be responded to promptly, (iii) the soft tissue cannot absorb enough energy, and (iv) the remaining energy surpasses the proximal femur strength [22].

3.1 Body Configuration

Body configuration can significantly affect the outcome of a fall [1], [21], [23]–[27]. A case-control analysis of a cohort study on community living older females (+65 years old) found the group with hip fracture were mainly fallen sideways, near the hip region [1]. Another study among 206 patients and 100 controls discovered that the majority of the patients had fallen directly to the side [21]. In both studies, the patients could not break their fall with their arm or hand, and an impact on the greater trochanter of the proximal femur has occurred. Similar findings were reported in two experimental studies.

Previous studies on fall kinematics suggested three body-angles to be relevant in the magnitude of the impact forces as a result of a sideways falling (Figure 3.1) [23], [24], [28]. The knee flexion angle was found to be on average 109 degrees [23], [28]. The trunk angle, which is the angle between the trunk and the vertical, was measured to be 17.3 degrees (SD = 11.5°) in an experimental fall study [23]. The same study found that a fall with an active muscle could increase the average trunk angle from 13.6 degrees (SD = 11.2°) to 21.8 degrees (SD = 10.4°). Another study on a larger cohort suggests an average trunk angle of 42 degrees when the hip impacts the ground after an initial hand or knee impact [24]. The last body angle is the anterior or posterior rotation of the pelvis (pelvis angle). A recent study explored the effect of variation of the pelvis angle on the generated internal forces measured on the femoral head using a hip impactor simulator [29]. It was found that a 10-degree anterior rotation of the pelvis can lead to the highest internal forces [29]. The experimental study on the 44 young subjects found that the average pelvis angle is 8 degrees (SD= 15) posterior rotation.

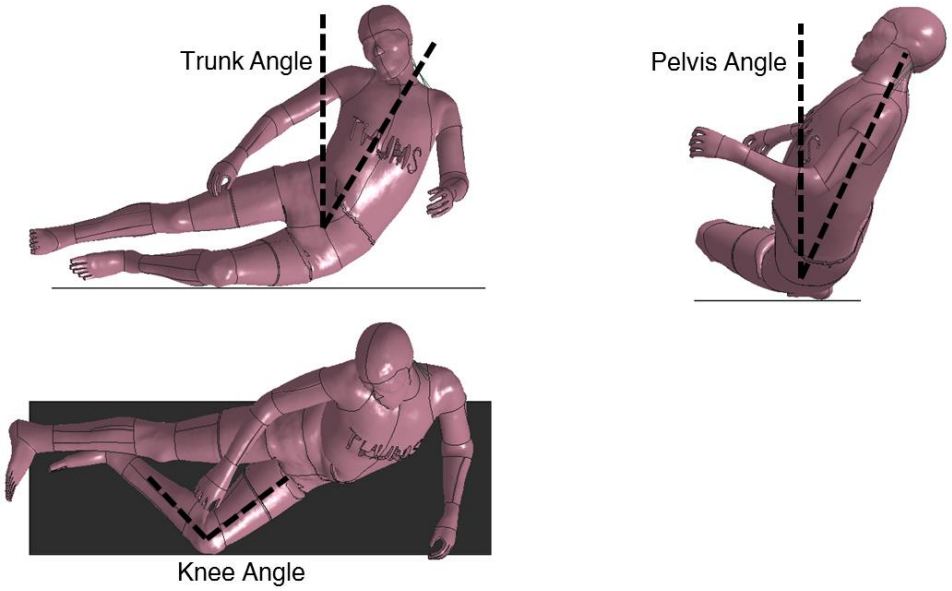

Figure 3.1. Different relevant body angles in a sideways fall incident

Finally, the hip velocity during sideways falls was reported on average 3.0 m/s [27]. The two experiments on young human volunteers reported similar range of falling velocities of 3.17 m/s (SD = 0.47) [23] and 3.01 m/s (SD = 0.83) [24].

3.2 Pelvis Segment

The human body's pelvis segment can be divided into three main sections, as shown in Figure 3.2: Internal soft tissues (Figure 3.2, a), bony tissues (Figure 3.2, b), and external soft tissues (Figure 3.2, c). The internal soft tissue consists of the soft tissues that are medial to the femur, such as pubic symphysis, ligaments, and cartilages. The bony tissue consists of the femur and pelvis. Finally, the external soft tissue consists of the muscular tissue covering the proximal femur, fat, and skin [30], [31].

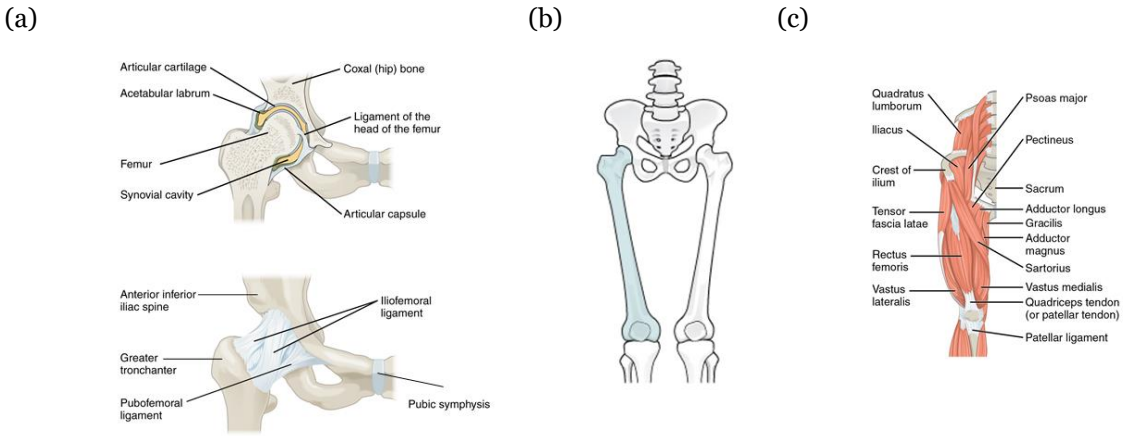

Figure 3.2. (a) internal soft tissues, (b) bony tissue, (c) external soft tissues (skin and fat were excluded), [32] (CC BY 4.0, Download for free at http://cnx.org/contents/14fb4ad7-39a1-4eee-ab6e-3ef2482e3e22@11.1.

The pubic symphysis is a cartilage tissue between the left and right pubic bone. The femoral head and the acetabulum form a ball and socket joint named the hip joint. There are articular cartilage and several ligaments responsible for increasing the hip joint's stability [30]. The proximal femur has three important geometric features: the femoral head attached to the acetabulum, the femoral neck, the region between the femoral head and femoral shaft, and the greater trochanter, which is located on the lateral and proximal side of the femur. The muscular tissue covers the greater trochanteric area of the proximal femur. A thin layer of fat and a layer of skin covers the muscles and bones and surrounds the pelvis segment.

In any impact to the side of the hip region, the external and internal soft tissues are participating in the force attenuation [33]–[35], and the bony tissue carries the rest of the impact forces [35], [36]. Thus, the soft tissue force attenuation capacity and the femoral strength are decisive parameters in the fall outcome.

3.2.1 Soft tissue

Soft tissues in the pelvis segment are the natural shock-absorbing elements that can reduce the impact forces [35], [37]–[40]. Previous studies on fall injury found that soft tissue thickness plays an important role in force attenuation [35], [38], [41], [42]. A previous study on 21 postmenopausal females and 42 age-matched controls revealed that the lower soft tissue thickness was associated with a higher risk of hip fracture [41]. Another study conducted on the femur surrogate and different soft tissue thicknesses indicated a 70 N decrease of internal forces measured on the femoral head for every 1 mm increase in the thickness [35]. Another numerical study proposed a power-law relationship

between the thickness and the impact force [38]. The soft tissue thickness measures in different previous studies reveal that the average thickness across different populations is 32 mm (SD = 23.2), and the average for a group with hip fracture reduces to 28.3 mm [43].

3.2.2 Bone tissue

After attenuation by soft tissue, the remaining impact forces are applied to the femur, which needs to resist against it with its strength. The femur consists of cortical and trabecular bones, and each of the bone types contributes to the femoral strength [44], [45]. There is a great deal of debate surrounding the contribution of the cortical and trabecular bone. Depending on the location on the proximal femur, loading condition, and age of the subjects, the cortical bone contribution can vary between 90 to 60 percent [44]–[47].

The cortical and trabecular bones have been modelled differently in different studies. It has been shown that the cortical bone has transverse isotropic mechanical properties [48]–[54]. The transverse direction is perpendicular to the shaft axis, and the longitudinal direction is along the direction of osteons [50].

4 Method

4.1.1 THUMS, a Whole-Body Model

The whole-body model used to simulate the complicated fall kinematics was THUMS v4.02. The THUMS v4.02 represented a medium-size adult male (50th percentile) with a weight of 76 kg and a height of 177 cm [17]. This version includes the skeletal system, brain, internal organs, and soft tissue (flesh). The original model was developed for the pedestrian and car occupant accidents; consequently, it was necessary to revise the model for required enhancements. First, the soft tissues' geometry and constitutive model, both the internal and external ones, were revised to become more representative of those tissues [55]–[63]. The constitutive material models were presented briefly (paper B). Then, the model was positioned in the different trunk and pelvis angles (paper A) and later were impacted to a rigid ground to evaluate the internal forces generated on the femoral head in each of the body configurations. The proximal femur's geometry and mechanical properties were also revised in Paper C to represent the elderly adults better. The small female model is homogenously scaled down (0.87) from the medium size male model (Figure 4.1).

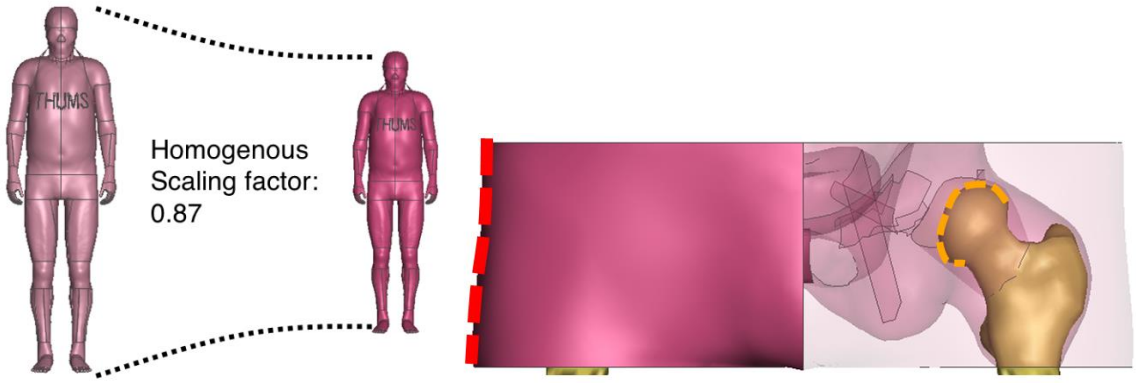

Figure 4.1. Left: Homogenous scaling of the small female model from the medium-size male model. Right: The external forces were measured on the impact side (red line), the internal forces were measured on the femoral head (orange line).

4.1.2 Force Evaluation in the FE Model

The fall-induced forces can be measured in several locations. When the impact forces in the segment models or whole-body models (paper B and E) were evaluated on the lateral side of the soft tissue (impact side), it was denoted as the external forces. In contrast, when the forces were evaluated on the femoral head, which is in contact with the acetabulum, it is denoted as internal forces (**Fel! Hittar inte referenskälla.**).

4.1.3 Detailed child full body model

The PIPER scalable HBM is a detailed child full body model able to describe the growth process and the variation in relevant anatomical regions for children (Fig. 4.2) [64], [65]. The baseline model describes the anatomy of an average 6YO child and has a total mass of 23 Kg. The anthropometric dimensions were normalized by nonlinear scaling using GEBOD regressions as reference. Overall, the model is composed of approximately 531,000 elements (including about 52,000 rigid elements) distributed into 353 parts describing the main anatomical structures.

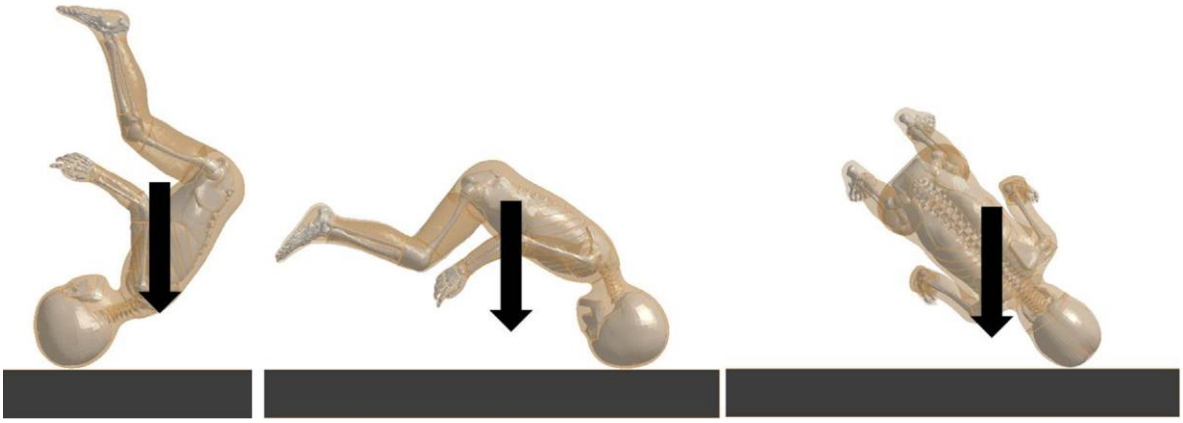

Figure 4.2. Simulations of three playground falls (back, front, side) led to occipital, frontal and parietal impact of the head, illustrated with the 3 YO model.

4.2 Bone Damage Model

The original material model for the cortical bone was elastic with symmetric failure modes. Given the large size of the femoral mesh and the whole-body model's complexity, the failure mode in which the corresponding element would be deleted seems to need improvement. The cortical bone was modeled using a transverse-isotropic model, and the asymmetry of the bone failure was considered using a simplified damage model.

4.3 Hyperelastic Material Models of Soft Tissue

The soft tissue is responsible for the force attenuation during a fall incident. Consequently, it was essential to implement a constitutive material model representing each of the soft tissues. Three material models were implemented to investigate the model with the best correlation to the experiments.

4.4 Asphalt Material Modeling

Bituminous mixtures with four different crumb rubber contents, namely 0%, 14%, 28%, and 33 % (in total weight) were produce at the University of Bologna, Italy within the Horison2020 project SAFERUP! Two mechanical testing sets were performed on the samples: non-destructive compression test and destructive compression test (4.3). The failure point in the destructive test was identified as a point where a visible deep crack was detected or when the force-deflection curves pass the maximum force. The non-destructive compression test applied a 1% strain with a displacement rate of 0.5 mm/min, and a displacement rate of 5 mm/min was applied during the destructive compression test. Later, the mechanical compression tests were used to evaluate Young's modulus of the samples and implement the stress-strain curves into the *MAT_SIMPLIFIED_RUBBER material model in LS-Dyna [66]. The material model is a simple model that automatically computes the Ogden functional [67] using the provided stress-strain curves.

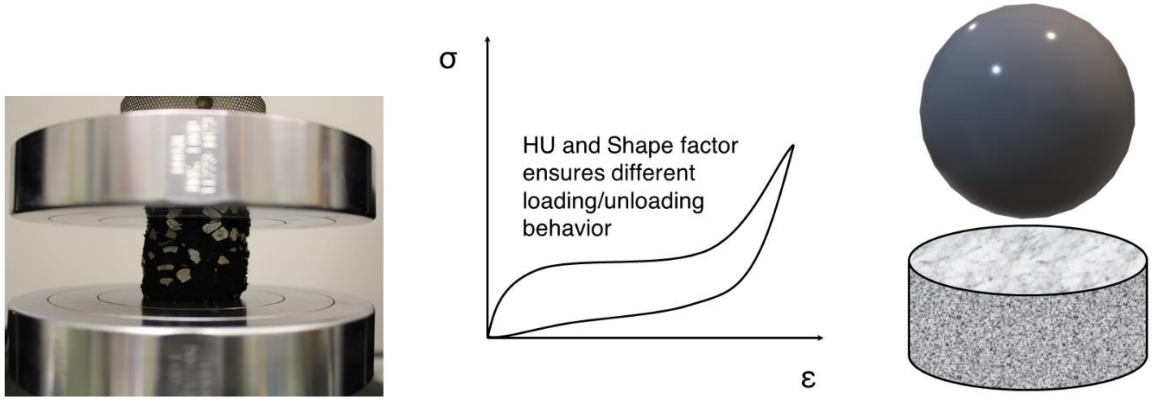

Figure 4.3. Left: An asphalt mixture during the compression test. Middle: A typical stress-strain curve for a *MAT_SIMPLIFIED_RUBBER model with non-zero HU/shape factors ensures a different unloading path [66]. Right: The HIC drop test setup.

The material model can govern the energy dissipation using two constants of hysteresis unloading (HU) and shape factor. These two constants were chosen to be 0.1 and 5, respectively (Figure 4.3). The material model for each asphalt mixture was validated using a standard HIC drop test [68]. The drop tests were performed using a hemispheric impactor with weight and diameter of 4.6 kg and 160 mm, which was released from different heights.

5 Results

5.1 Paper A: Body Configuration

The whole-body model was positioned in the trunk angles ranging from 10 to 80 degrees and the pelvis angles ranging from -20 to +20 degrees. The trunk angle's highest internal forces occurred in the 10 degrees' trunk angle for females and males (Figure 5.1). Similarly, the highest internal forces for the pelvis angle occurred in +10 degrees' pelvis rotation. The small-size female model (weight 56 kg, height 156 cm) experienced relatively lower internal forces than the medium-size male model (weight 76 kg, height 177 cm) since it had a lower body weight.

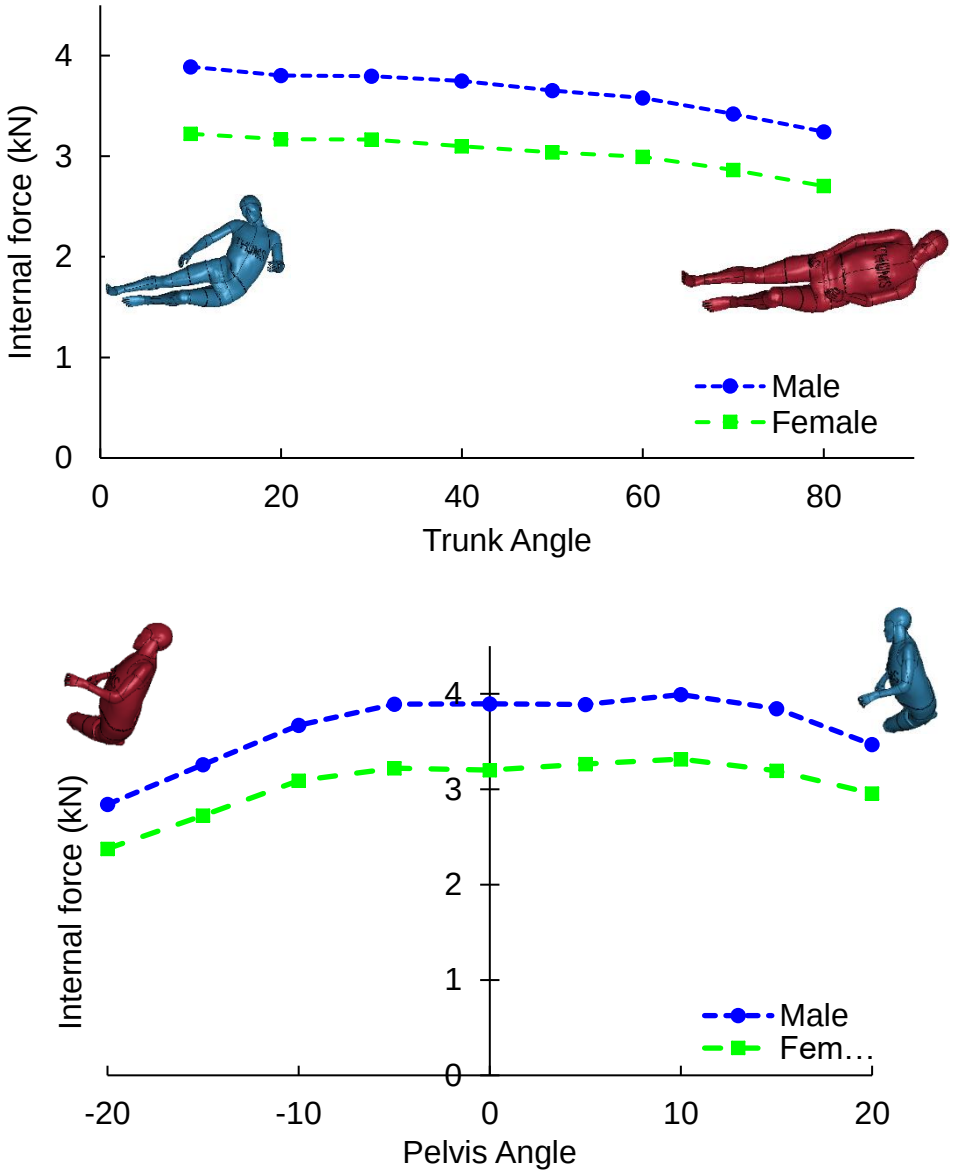

Figure 5.1. internal forces measured in the different trunk and pelvis angles for a medium-size male and a small-size female. Upper: Comparison of internal forces in different trunk angles. The internal forces decrease as the trunk angle reaches the horizontal body configuration. Lower: Comparison of the internal forces in different pelvis angles when the trunk angle was fixed to 10 degrees. The internal force reaches the maximum value for both sexes at a pelvis angle of +10 degrees.

5.2 Paper B: Objective Assessment of Soft Tissue Material Model

The CORA ratings for various constitutive models can be found in paper B in the appendix. Three models with the highest ratings were selected from the pelvis segment model to implement in the whole-body model. The highest CORA rating among the three selected models occurred in the Ogden model based on the experimental study by Van Loocke et al. [69], [70].

5.3 Paper C: Aging Bone

The changes in the proximal femur are age and sex-dependent. The geometrical changes caused a 25 N/decade of age increase in the femoral strength for males, whereas it caused a 116 N/decade decrease for the females. The mechanical properties change affected males and females differently even though the mechanical properties changes were implemented similarly. While the femoral strength decreased by about 354 N/decade for males, it only reduced 225 N/decade for females. Finally, the combination of the geometrical changes and mechanical properties changes in both sexes caused a 373 N/decade and 368 N/decade reductions in femoral strength for the males and females. It is noteworthy that the males experience a 7 percent decrease in femoral strength, whereas females experience an 11 percent reduction.

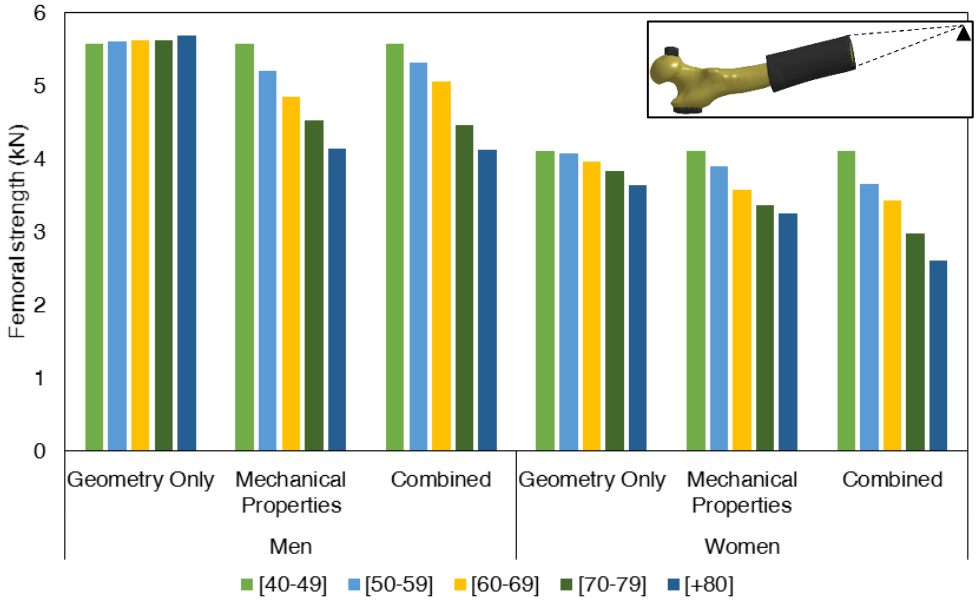

Figure 5.2. The femoral strength changes in the males and females due to separate and combined changes in the proximal femur's geometry and mechanical properties.

5.4 Paper D: Risk of Head Injury on the Rubberized Asphalt

Bituminous mixtures with four different crumb rubber contents, namely 0%, 14%, 28%, and 33 % (in total weight) produced at the University of Bologna, Italy within the Horison2020 project SAFERUP! and a polyurethane binder-based rubber playground material were used to assess the ability to reduce the head injury risk, i.e., skull fracture and concussion for two real case accidents. In the bicycle accident case, the playground material had a skull fracture risk reduction of 94 percent compared to 0 wt% asphalt, whereas the bituminous 33 wt% rubber mixture had a 70 percent reduction compared to 0 wt% asphalt (Figure 5.3). The brain concussion risk reduction was not as significant as for the

skull fracture. The bituminous sample with 33 wt% rubber content had a concussion risk of 80 percent, similar to the playground material with 83.

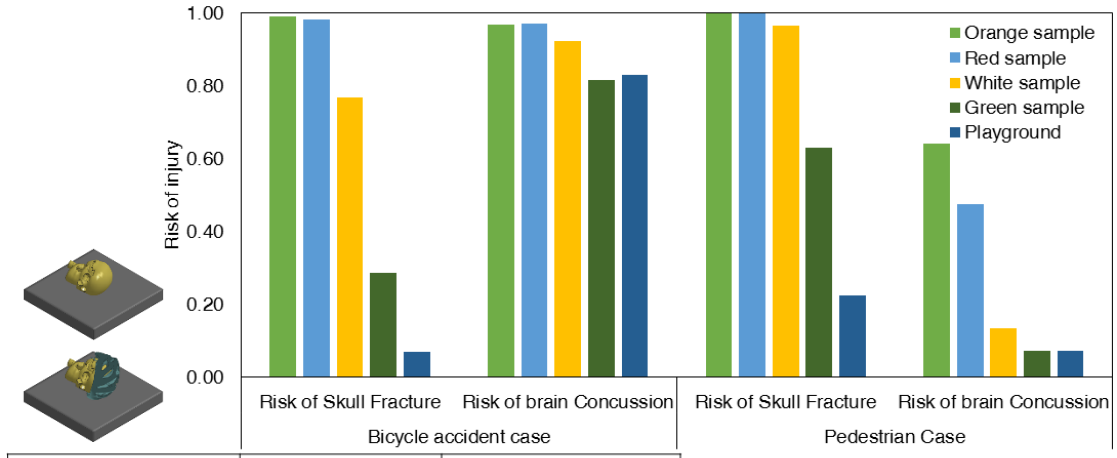

Orange sample/with helmet	0.06	0.51
Green sample/with helmet	0.04	0.57

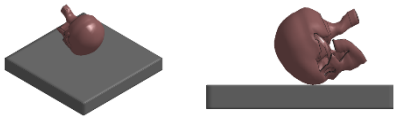

Figure 5.3. The skull fracture risk [71] and the brain concussion risk [72] were evaluated for the bicycle and pedestrian accident cases when impacting the three asphalt mixtures and the reference materials.

In the pedestrian case, the risk of skull fracture for the playground material was 23 percent compared to the reference non-rubberized asphalt mixture which had a risk of 97 percent. For the bituminous 33 wt% rubber asphalt mixture the risk of skull fracture was 63 percent. For pedestrian concussion, all rubber containing samples had significantly lower risks compared to asphalt with 0 wt% rubber. For the asphalt with 0 wt% rubber the risk of concussion was 63 percent. For the playground material and the bituminous 33 wt% rubber asphalt mixture the risk was 6%, for the 28 wt% rubber asphalt it was 12 percent and for the 14 wt% rubber asphalt it was 47% (Figure 5.3).

5.5 Paper E: Risk of Hip Injury on the Rubberized Asphalt

The body posture which led to the highest internal forces in paper A was selected for simulation of the fall incident (Figure 5.4). In addition to the samples used in Figure 5.4, another more compliant playground material was also simulated. The hip fracture risk was evaluated for the elderly male and elderly female falling on different materials. The internal forces reduced around 15 percent for both male and female models. According to the internal forces, the risk of hip fracture for an elderly male and an elderly female was computed. The potential risk of hip fracture for males was considerably low compared to females (about half). While the hip fracture risk was reduced from around 64 percent for the 0 wt% asphalt to around 49 percent with the bituminous 33 wt% rubber content mixture in females, it reduced from around 36 percent for 0 wt% asphalt to 24 percent in males. With the compliant playground material, the hip fracture risk of was 33 percent for females and 15 percent for males (Figure 5.4).

(a)

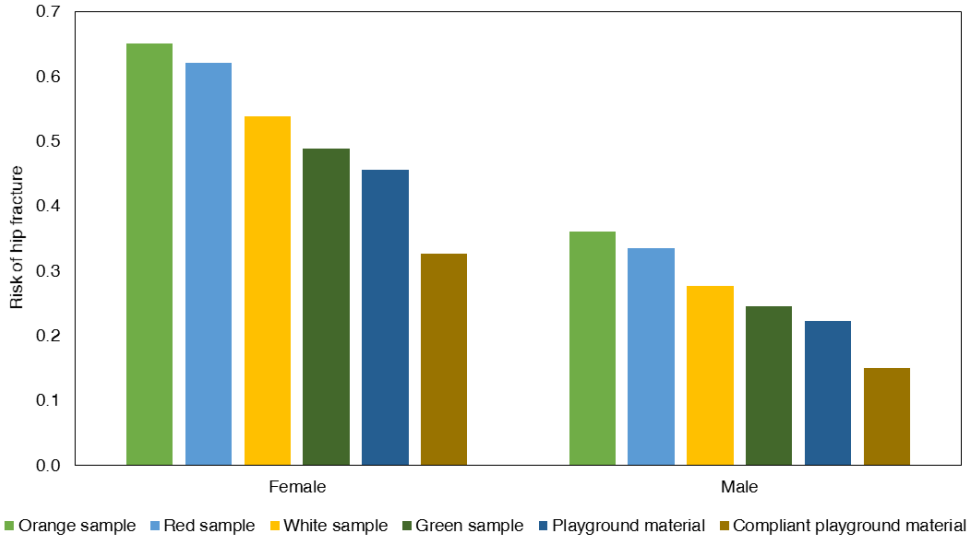

(b)

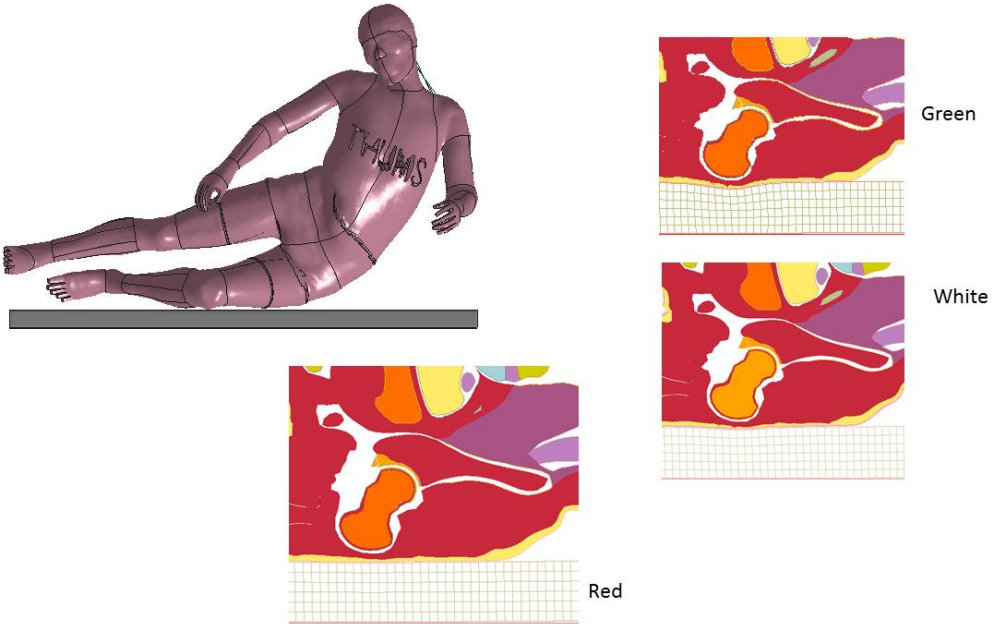

Figure 5.4. (a) the hip fracture risks [73] were evaluated for the elderly males and elderly females when falling on the three asphalt mixtures and the reference materials, (b) the maximum deflection of the asphalt mixtures during a sideways fall.

5.6 Evaluation of falls on playgrounds for children

The analysis highlights the age dependence of head injuries in children due to playground falls and the youngest have a higher risk of brain injury and skull fracture [64], [65]. Further, the results provide the first biomechanical evidence guiding age-dependent injury thresholds for playground testing standards. The results also have direct implications for novel designs of playground materials for a better protection of children from TBIs. Only making the playground material thicker and more compliant is not sufficient. This study represents the first initiative of using full body human body models of children as a new tool to improve playground testing standards and to better protect the children at playgrounds.

A question is: Can a softer playground protect the brain? Therefore, a softer playground material is tested, and for comparison a stiff material is also tested. With the same impact condition, a softer playground material significantly reduces linear acceleration and consequently HIC, which in turn largely reduces skull bone stress, but the MPS in the brain are still above 0.3 especially for a side impact (Fig. 5.5). For a front impact, a soft material leads to a slight decrease in MPS in smaller ages (1.5YO, 3YO and 6YO), but the older ages do not benefit from a soft material, on the contrary, the MPS is slightly increased unexpectedly. For back and side impact, a soft material in general also leads to unexpected larger MPS than the baseline (Fig. 5.5a). The 1st principal G-L strain distribution is captured when maximum value occurs, illustrated with a 1.5YO (Fig. 5.5b) and a 10YO (Fig. 5.5c) side impact which has largest value of the three directions. The larger MPS caused by a softer material seems to be caused by a rotation allowed during the impact compared with the baseline. The results also highlight that more compliant playgrounds would reduce the risk of skull fractures but not necessarily brain injuries.

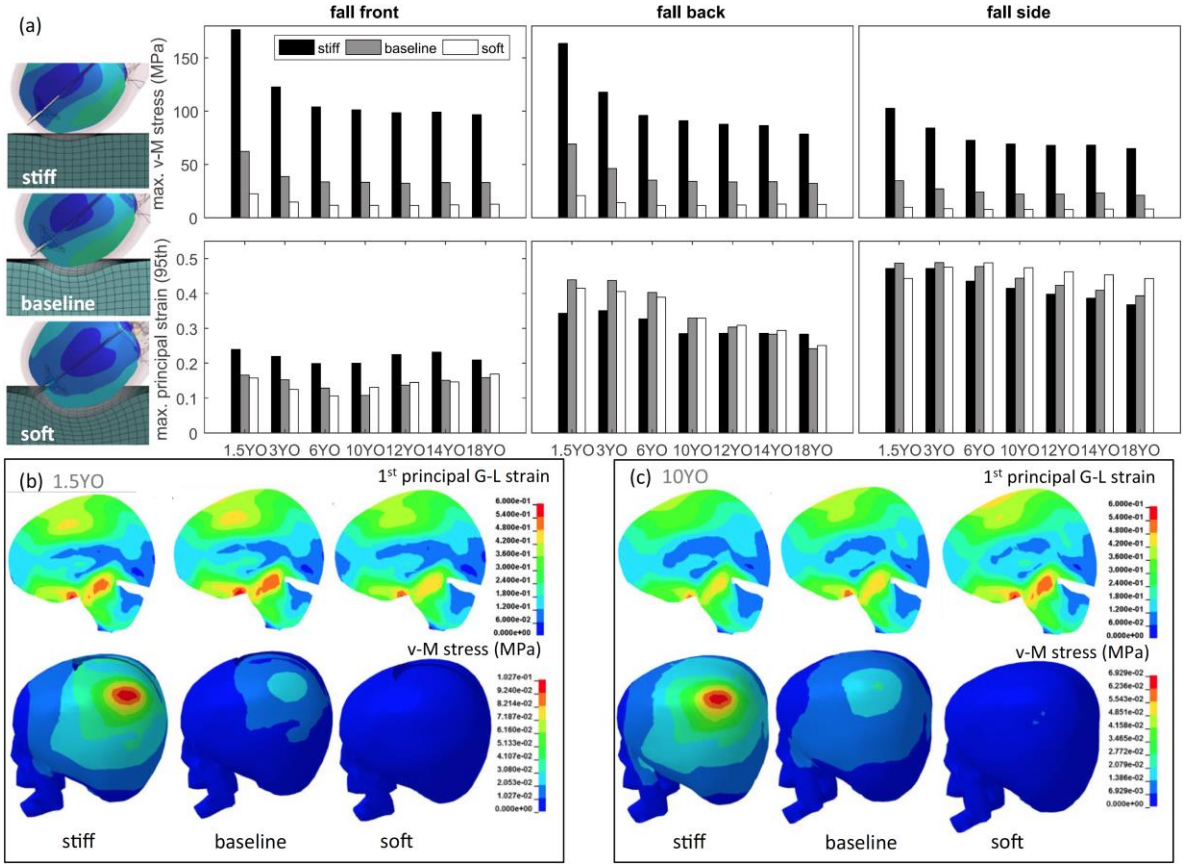

Figure 5.5. (a) Bar plots show the influence of impact direction and playground stiffness on MPS in the brain (row 1) and von-Mises skull stress (row 2). Image on the left captured at maximum indentation depth of the playground to visually illustrate the softness of a baseline the tested stiff and soft playground material, a 1.5YO side impact is shown in the illustration. Sagittal plane shows the distribution of 1st principal G-L strain when maximum value occurs; skull stress distribution captured when maximum value occurs for the 1.5YO side impact (b) and the 10YO side impact (c).

6 Future Work

Replacing traditional asphalt with rubber containing materials decreases injuries for pedestrian and cyclists. Comparing bituminous mixtures with four different crumb rubber contents 0%, 14%, 28%, and 33 %, shows that the injury risk reduction for all injury types is increasing with increasing rubber content. Largest effect is obtained for pedestrian concussion where the bituminous 33 wt% rubber mixture has an estimated risk of 6 percent compared to 63 percent for the 0% rubber mixture. For this injury and mobility type even the lowest rubber content reduces the injury risk significantly. Second largest injury reduction effect is obtained for cyclist skull fracture, which for the bituminous 33 wt% rubber mixture has an estimated risk of 29 percent compared to 100 percent for the 0% rubber mixture. Selecting the body posture which led to the highest internal forces for hip injury simulation show that the bituminous 33 wt% rubber mixture has an estimated risk of 48 percent compared to 64 percent for the 0% rubber mixture for the female model and 24 percent compared to 36 percent for the male. For hip injuries a compliant playground model further reduces these values to 32 percent for the female and 15 percent for the male. In addition to more diverse asphalt mixtures, it is necessary to study the locomotion, mobility, and balance over these new asphalt mixtures. There is a need for a thorough optimization study to maximize the soft asphalt injury prevention capacity while the balance, locomotion, durability, environmental friendliness of the asphalt mixture kept within a reasonable threshold. Identification of the parameters needed for the optimization and the temperature effects on injury prevention capacity of the asphalt mixtures are on-going. It is known that falls are also common during winter when the mechanical properties of the asphalt mixtures could be affected by this parameter as well [3]. Further suggestion is to also consider the combined effect with body protectors, especially for the elderly osteoporotic patients.

7 Budget

Total project cost

4,500,000 SEK

Detailed budget

Doctoral student at KTH 100% including travel, materials and administration 201606-202012: 3,600,000 SEK

Researcher at RISE 20% including travel, materials and administration 201606-202012: 900,000 SEK

A doctoral student was employed at KTH to focus on biomechanical fall injury models which is summarized on a doctoral thesis to be defended during autumn 2021.

A researcher at RISE worked on the project for developing biomechanically based certification tests for soft asphalt.

Dissemination of results and implementation

We have presented our results in national and international conferences in the field of damage biomechanics. Five scientific publications and a doctoral dissertation have been written, which can have a great impact in the field. However, the greatest impact is still the one made through the practical implementation.

Theses resulting from the project:

Sahandifar, P. (2021). Finite Element Modeling and Biomechanical Analysis of Fall Injuries. (Doctoral dissertation, KTH).

Peer-reviewed journal Publications resulting from the project:

Sahandifar P., Makoundou C., Fahlstedt M., Sangiorgi C., Johansson K., Wallqvist V., Kleiven, S. (2021). A rubberized impact absorbing pavement can prevent head injuries in vulnerable road users, a bicycle and a pedestrian accident case study. (manuscript).

Sahandifar, P., & Kleiven, S. (2021). Influence of nonlinear soft tissue modeling on the external and internal forces during lateral hip impacts. *Journal of the Mechanical Behavior of Biomedical Materials*, 104743.
https://www.sciencedirect.com/science/article/pii/S175161612100388X

Sahandifar, P., & Kleiven, S. (2021). Separate and combined effects of geometrical and mechanical properties changes due to aging on the femoral strength in men and women. *Frontiers in Mechanical Engineering*, *7*, 50.
https://www.frontiersin.org/articles/10.3389/fmech.2021.691171/full?utm_source=S-TWT&utm_medium=SNET&utm_campaign=ECO_FMECH_XXXXXXXX_auto-dlvrit

Kleiven, S., Sahandifar P. (2021). Upright torso and slight anterior rotation of pelvis causes the highest internal forces at the proximal femur during sideways falls. (manuscript).

Sahandifar P., Wallqvist V., Kleiven, S. (2021). Rubberized impact absorbing pavement reduces the hip fracture risk. (manuscript).

Peer-reviewed conference presentations resulting from the project:

Sahandifar P., Kleiven, S. (2018). Studying the age effect on fall induced hip fracture using an orthotropic continuum damage model (Short communication). International Research Council on the Biomechanics of Injury, IRCOBI, 11-12 September, Athen Greece.

Sahandifar P., Wallqvist V., Kleiven, S. (2020). Competence of soft asphalt for prevention of the fall induced injuries among vulnerable road users In *Transportforum 2020, Väg-och transportforskningsinstitutet, VTI, Linköping, 8-9 januari*. http://vti.diva-portal.org/smash/get/diva2:1411216/FULLTEXT01.pdf

8 References

[1] M. C. Nevitt and S. R. Cummings, "Type of Fall and Risk of Hip and Wrist Fractures: The Study of Osteoporotic Fractures," *J. Am. Geriatr. Soc.*, vol. 41, no. 11, pp. 1226–1234, Nov. 1993.

[2] J. P. Empana, P. Dargent-Molina, and G. Bréart, "Effect of Hip Fracture on Mortality in Elderly Women: The EPIDOS Prospective Study," *J. Am. Geriatr. Soc.*, vol. 52, no. 5, pp. 685–690, May 2004.

[3] Swedish Civil Contingencies Agency (MSB), "Social Costs of Accidents in Sweden," pp. 1–29, 2012.

[4] S. R. Cummings and L. J. Melton, "Osteoporosis I: Epidemiology and outcomes of osteoporotic fractures," *Lancet*, vol. 359, no. 9319. Elsevier Limited, pp. 1761–1767, 18-May-2002.

[5] J. A. Grisso, G. Y. Chiu, G. Maislin, W. C. Steinmann, and J. Portale, "Risk factors for hip fractures in men: A preliminary study," *J. Bone Miner. Res.*, vol. 6, no. 8, pp. 865–868, 1991.

[6] P. Kannus, J. Parkkari, H. Sievänen, A. Heinonen, I. Vuori, and M. Järvinen, "Epidemiology of hip fractures," in *Bone*, 1996, vol. 18, no. 1 SUPPL., pp. S57–S63.

[7] Centers for Disease Control and Prevention, "STEADI - Older Adult Fall Prevention | CDC Injury Center," *centers for disease control and prevention*, 2018. [Online]. Available: https://www.cdc.gov/steadi/materials.html. [Accessed: 28-Mar-2018].

[8] The Swedish Transport Administration, *Analysis of Road Safety Trends 2017*. The Swedish Transport Administration, 2018.

[9] A. Santacreu, "Safer City Streets Global Benchmarking for Urban Road Safety," Paris, Jan. 2018.

[10] World Health Organization (WHO), "Global Status Report on Road Safety 2018: Summary," Geneva, 2018.

[11] M. Rizzi, H. Stigson, and M. Krafft, "Cyclist Injuries Leading to Permanent Medical Impairment in Sweden and the Effect of Bicycle Helmets | Enhanced Reader," in *IRCOBI Conference*, 2013, pp. 412–423.

[12] M. Fahlstedt, P. Halldin, and S. Kleiven, "The protective effect of a helmet in three bicycle accidents - A finite element study," *Accid. Anal. Prev.*, vol. 91, pp. 135–143, Jun. 2016.

[13] V. Wallqvist, G. Kjell, E. Cupina, L. Kraft, C. Deck, and R. Willinger, "New functional pavements for pedestrians and cyclists," *Accid. Anal. Prev.*, vol. 105, no. May, pp. 52–63, Aug. 2017.

[14] V. Wallqvist and L. Kraft, "Prototype bike lanes - placement practices and properties," in *3rd international conference on best practices for concrete pavements*, 2015, no. October 2015.

[15] M. Fahlstedt *et al.*, "Influence of impact velocity and angle in a detailed reconstruction of a bicycle accident," in *IRCOBI Conference Proceedings - International Research Council on the Biomechanics of Injury*, 2012, pp. 787–799.

[16] M. Iwamoto and Y. Nakahira, "Development and Validation of the Total HUman Model for Safety (THUMS) Version 5 Containing Multiple 1D Muscles for Estimating Occupant Motions with Muscle Activation During Side Impacts," in *SAE Technical Papers*, 2015, no. November.

[17] M. Iwamoto, Y. Kisanuki, I. Watanabe, K. Furusu, and K. Miki, "Development of a finite element model of the total human model for safety (THUMS) and application to injury reconstruction," in *International Research Council on Biomechanics of Injury*, 2002, pp. 31–42.

[18] A. J. Golman, K. A. Danelson, L. E. Miller, and J. D. Stitzel, "Injury prediction in a side impact crash using human body model simulation," *Accid. Anal. Prev.*, 2014.

[19] S. L. Schoell *et al.*, "Development and Validation of an Older Occupant Finite Element Model of a Mid-Sized Male for Investigation of Age-related Injury Risk," in *Stapp car crash journal*, 2015, vol. 59, no. December, p. 359.

[20] M. L. Davis, B. Koya, J. M. Schap, and F. S. Gayzik, "Development and Full Body Validation of a 5th Percentile Female Finite Element Model," *SAE Tech. Pap.*, vol. 60, no. November, pp. 509–544, 2016.

[21] J. Parkkari *et al.*, "Majority of hip fractures occur as a result of a fall and impact on the greater trochanter of the femur: A prospective controlled hip fracture study with 206 consecutive patients," *Calcif. Tissue Int.*, vol. 65, no. 3, pp. 183–187, 1999.

[22] S. R. Cummings and M. C. Nevitt, "A hypothesis: The causes of hip fractures," *Journals Gerontol.*, vol. 44, no. 4, 1989.

[23] A. J. Van Den Kroonenberg, W. C. Hayes, and T. A. McMahon, "Hip impact velocities and body configurations for voluntary falls from standing height," *J. Biomech.*, vol. 29, no. 6, pp. 807–811, Jun. 1996.

[24] F. Feldman and S. N. Robinovitch, "Reducing hip fracture risk during sideways falls: Evidence in young adults of the protective effects of impact to the hands and stepping," *J. Biomech.*, vol. 40, no. 12, pp. 2612–2618, Jan. 2007.

[25] M. N. Sarvi, Y. Luo, P. Sun, and J. Ouyang, "Experimental Validation of Subject-Specific Dynamics Model for Predicting Impact Force in Sideways Fall," *J. Biomed. Sci. Eng.*, vol. 7, no. 7, pp. 405–418, 2014.

[26] W. C. Hayes, E. R. Myers, S. N. Robinovitch, A. Van Den Kroonenberg, A. C. Courtney, and T. A. McMahon, "Etiology and prevention of age-related hip fractures," *Bone*, vol. 18, no. 1, pp. S77–S86, Jan. 1996.

[27] M. Nasiri Sarvi and Y. Luo, "Sideways fall-induced impact force and its effect on hip fracture risk: a review," *Osteoporos. Int.*, vol. 28, no. 10, pp. 2759–2780, Oct. 2017.

[28] I. Fleps *et al.*, "A novel sideways fall simulator to study hip fractures ex vivo," *PLoS One*, vol. 13, no. 7, p. e0201096, Jul. 2018.

[29] W. J. Choi and S. N. Robinovitch, "Effect of pelvis impact angle on stresses at the femoral neck during falls," *J. Biomech.*, vol. 74, pp. 41–49, Jun. 2018.

[30] Henry Gray, *Anatomy of the Human Body*. Philadelphia: Lea & Febiger, 1918.

[31] J. G. Betts *et al.*, *Anatomy and phsiology*, vol. 53, no. 9. 2017.

[32] OpenStax College OpenStax CNX, "Anatomy and Physiology," *OpenStax CNX*. [Online]. Available: http://cnx.org/contents/14fb4ad7-39a1-4eee-ab6e-3ef2482e3e22@11.1. [Accessed: 30-Jan-2021].

[33] P. Sahandifar and S. Kleiven, "Influence of nonlinear soft tissue modeling on the external and internal forces during sideways falls."

[34] W. J. Choi, P. A. Cripton, and S. N. Robinovitch, “Effects of hip abductor muscle forces and knee boundary conditions on femoral neck stresses during simulated falls,” *Osteoporos. Int.*, vol. 26, no. 1, pp. 291–301, Jan. 2015.

[35] S. N. Robinovitch, T. A. McMahon, and W. C. Hayes, “Force attenuation in trochanteric soft tissues during impact from a fall,” *J. Orthop. Res.*, vol. 13, no. 6, pp. 956–962, 1995.

[36] M. N. Sarvi, “Assessment of Hip Fracture Risk by a Two- Level Subject-Specific Biomechanical Model,” 2015.

[37] S. N. Robinovitch, W. C. Hayes, and T. A. McMahon, “Prediction of Femoral Impact Forces in Falls on the Hip,” *J. Biomech. Eng.*, vol. 113, no. 4, pp. 366–374, Nov. 1991.

[38] S. Majumder, A. Roychowdhury, and S. Pal, “Effects of trochanteric soft tissue thickness and hip impact velocity on hip fracture in sideways fall through 3D finite element simulations,” *J. Biomech.*, vol. 41, no. 13, pp. 2834–2842, Sep. 2008.

[39] S. Majumder, A. Roychowdhury, and S. Pal, “Hip fracture and anthropometric variations: Dominance among trochanteric soft tissue thickness, body height and body weight during sideways fall,” *Clin. Biomech.*, vol. 28, no. 9–10, pp. 1034–1040, Nov. 2013.

[40] I. C. Levine, L. E. Minty, and A. C. Laing, “Factors that influence soft tissue thickness over the greater trochanter: Application to understanding hip fractures,” *Clin. Anat.*, vol. 28, no. 2, pp. 253–261, Mar. 2015.

[41] M. L. Bouxsein, P. Szulc, F. Munoz, E. Thrall, E. Sornay-Rendu, and P. D. Delmas, “Contribution of trochanteric soft tissues to fall force estimates, the factor of risk, and prediction of hip fracture risk,” *J. Bone Miner. Res.*, vol. 22, no. 6, pp. 825–831, Mar. 2007.

[42] W. J. Choi, C. M. Russell, C. M. Tsai, S. Arzanpour, and S. N. Robinovitch, “Age-related changes in dynamic compressive properties of trochanteric soft tissues over the hip,” *J. Biomech.*, vol. 48, no. 4, pp. 695–700, Feb. 2015.

[43] F. L.-S. Goh, “Wearable Hip Protectors : Validation of a Novel Test System and Evaluation Utilizing Pressure Sensing Methods by,” 2017.

[44] F. Johannesdottir, E. Thrall, J. Muller, T. M. Keaveny, D. L. Kopperdahl, and M. L. Bouxsein, “Comparison of non-invasive assessments of strength of the proximal femur,” *Bone*, vol. 105, pp. 93–102, Dec. 2017.

[45] S. Nawathe, B. P. Nguyen, N. Barzanian, H. Akhlaghpour, M. L. Bouxsein, and T. M. Keaveny, “Cortical and trabecular load sharing in the human femoral neck,” *J. Biomech.*, vol. 48, no. 5, pp. 816–822, 2015.

[46] S. L. Manske *et al.*, “Cortical and trabecular bone in the femoral neck both contribute to proximal femur failure load prediction,” *Osteoporos Int*, vol. 20, pp. 445–453, 2009.

[47] G. Holzer *et al.*, “Hip Fractures and the Contribution of Cortical Versus Trabecular Bone to Femoral Neck Strength,” *J. Bone Miner. Res.*, vol. 2424, no. 3, pp. 468–474, Mar. 2009.

[48] R. B. B. Ashman, S. C. C. Cowin, W. C. C. Van Buskirk, J. C. Rice, and J. C. Rice+, “A continuous wave technique for the measurement of the elastic properties of cortical bone,” *J. Biomech.*, vol. 17, no. 5, pp. 349–361, Jan. 1984.

[49] D. T. Reilly, A. H. Burstein, and V. H. Frankel, “The elastic modulus for bone,” *J. Biomech.*, vol. 7, no. 3, pp. 271–275, May 1974.

[50] D. T. Reilly and A. H. Burstein, “The elastic and ultimate properties of compact bone tissue,”

J. Biomech., vol. 8, no. 6, pp. 393–405, Jan. 1975.

[51] J. Currey, "Incompatible mechanical properties in compact bone," *J. Theor. Biol.*, vol. 231, no. 4, pp. 569–580, Dec. 2004.

[52] H. H. Bayraktar, E. F. Morgan, G. L. Niebur, G. E. Morris, E. K. Wong, and T. M. Keaveny, "Comparison of the elastic and yield properties of human femoral trabecular and cortical bone tissue," *J. Biomech.*, vol. 37, no. 1, pp. 27–35, 2004.

[53] C. H. Turner, J. Rho, Y. Takano, T. Y. Tsui, and G. M. Pharr, "The elastic properties of trabecular and cortical bone tissues are similar: results from two microscopic measurement techniques," *J. Biomech.*, vol. 32, pp. 437–441, 1999.

[54] W. S. Enns-Bray, J. S. Owoc, K. K. Nishiyama, and S. K. Boyd, "Mapping anisotropy of the proximal femur for enhanced image based finite element analysis," *J. Biomech.*, vol. 47, pp. 3272–3278, 2014.

[55] L. Khorashadi, J. M. Petscavage, and M. L. Richardson, "Postpartum symphysis pubis diastasis," *Radiol. Case Reports*, vol. 6, no. 3, p. 542, 2011.

[56] A. Pedrazzini, R. Bisaschi, R. Borzoni, D. Simonini, and A. Guardoli, "Post partum diastasis of the pubic symphysis: A case report," *Acta Biomed. l'Ateneo Parm.*, vol. 76, no. 1, pp. 49–52, 2005.

[57] Z. Li, J. E. Kim, J. S. Davidson, B. S. Etheridge, J. E. Alonso, and A. W. Eberhardt, "Biomechanical response of the pubic symphysis in lateral pelvic impacts: A finite element study," *J. Biomech.*, vol. 40, no. 12, pp. 2758–2766, 2007.

[58] K. A. Athanasiou, A. Agarwal, and F. J. Dzida, "Comparative study of the intrinsic mechanical properties of the human acetabular and femoral head cartilage," *J. Orthop. Res.*, vol. 12, no. 3, pp. 340–349, 1994.

[59] S. S. Chen, Y. H. Falcovitz, R. Schneiderman, A. Maroudas, and R. L. Sah, "Depth-dependent compressive properties of normal aged human femoral head articular cartilage: Relationship to fixed charge density," *Osteoarthr. Cartil.*, vol. 9, no. 6, pp. 561–569, 2001.

[60] A. E. Anderson, B. J. Ellis, S. A. Maas, and J. A. Weiss, "Effects of idealized joint geometry on finite element predictions of cartilage contact stresses in the hip," *J. Biomech.*, 2010.

[61] J. Hewitt, F. Guilak, R. Glisson, and T. P. Vail, "Regional material properties of the human hip joint capsule ligaments," *J. Orthop. Res.*, vol. 19, no. 3, pp. 359–364, 2001.

[62] J. D. Hewitt, R. R. Glisson, F. Guilak, and T. P. Vail, "The mechanical properties of the human hip capsule ligaments," *J. Arthroplasty*, vol. 17, no. 1, pp. 82–89, 2002.

[63] J. Li, T. D. Stewart, Z. Jin, R. K. Wilcox, and J. Fisher, "The influence of size, clearance, cartilage properties, thickness and hemiarthroplasty on the contact mechanics of the hip joint with biphasic layers," *J. Biomech.*, vol. 46, no. 10, pp. 1641–1647, 2013.

[64] X. Li and S. Kleiven, "Improved safety standards are needed to better protect younger children at playgrounds," *Sci. Rep.*, vol. 8Li, X., K, no. 1, pp. 1–12, 2018.

[65] M. Fahlstedt, S. Kleiven, and X. Li, "Current playground surface test standards underestimate brain injury risk for children," *J. Biomech.*, vol. 89, pp. 1–10, 2019.

[66] LSTC, *LS-DYNA R12 Keywords Manual, version 971*, vol. II. LIVERMORE SOFTWARE TECHNOLOGY (LST), AN ANSYS COMPANY, 2020.

[67] R. Ogden, *Non-linear elastic deformations*. 1984.

[68] SIS, *Standard - Impact attenuating playground surfacing - Methods of test for determination of impact attenuation SS-EN 1177:2018+AC*. 2019.

[69] M. Van Loocke, C. G. Lyons, and C. K. Simms, "Viscoelastic properties of passive skeletal muscle in compression: Stress-relaxation behaviour and constitutive modelling," *J. Biomech.*, vol. 41, no. 7, pp. 1555–1566, 2008.

[70] M. Van Loocke, C. G. Lyons, and C. K. Simms, "A validated model of passive muscle in compression," *J. Biomech.*, vol. 39, no. 16, pp. 2999–3009, 2006.

[71] P. Chan, S. Diego, P. Rigby, E. Takhounts, and J. Zhang, "Development of a generalized linear skull fracture criterion," no. June 2015, 2007.

[72] S. Kleiven, "Predictors for Traumatic Brain Injuries Evaluated through Accident Reconstructions," in *SAE Technical Papers*, 2007, vol. 2007-Octob, no. October.

[73] S. Kleiven, "Hip fracture risk functions for elderly men and women in sideways falls," *J. Biomech.*, vol. 105, p. 109771, May 2020.